Published in final edited form as:
Magn Reson Imaging. 2013 December ; 31(10): 1668–1676. doi:10.1016/j.mri.2013.05.012.

A comparative study of magnetic resonance venography techniques for the evaluation of the internal jugular veins in multiple sclerosis patients☆

M. Tamizur Rahman[a], **Sean K. Sethi**[a,*], **David T. Utriainen**[a], **J. Joseph Hewett**[b], and **E. Mark Haacke**[a,c]

[a]Magnetic Resonance Innovations, Inc., Detroit, MI, USA

[b]Pacific Interventionalists, Newport Beach, CA, USA

[c]Wayne State University, Detroit, MI, USA

Abstract

Background and Purpose—The use of magnetic resonance imaging (MRI) to assess the vascular nature of diseases such as multiple sclerosis (MS) is a growing field of research. This work reports on the application of MR angiographic (MRA) and venographic (MRV) techniques in assessing the extracranial vasculature in MS patients.

Materials and Methods—A standardized MRI protocol containing 2D TOF-MRV and dynamic 3D contrast-enhanced (CE) MRAV was run for 170 MS patients and 40 healthy controls (HC). The cross-sectional area (CSA) of the internal jugular veins (IJVs) was measured at three neck levels in all subjects for both MRV techniques to determine the presence of venous stenoses. All data were analyzed retrospectively.

Results—For the values where both methods showed signal, the 3D method showed larger CSA measurement values compared to 2D methods in both IJVs, in both MS and HC subjects which was confirmed with student paired t-tests. Of the 170 MS patients, 93 (55%) in CE-MRAV and 103 (61%) in TOF-MRV showed stenosis in at least one IJV. The corresponding numbers for the 40 HC subjects were 2 (5%) and 4 (10%), respectively. Carotid ectasias with IJV stenosis were seen in 26 cases (15%) with 3D CE-MRAV and were not observable with 2D TOF-MRV. Carotid ectasias were not seen in the HC group. In the 2D TOF-MRV data, banding of the IJVs related to slow flow was seen in 58 (34%) MS cases and in no HC cases. MS patients showed lower average CSAs than the HC subjects.

Conclusion—The 3D CE MRAV depicted the vascular anatomy more completely than the 2D TOF-MRV. However, the 3D CE MRAV does not provide any information about the flow characteristics which are indirectly available in the 2D TOF-MRV in those cases where there is slow flow.

Keywords

MR venography; Multiple sclerosis; Extracranial venous system; Internal jugular veins; Time-of-flight; Dynamic 3D contrast-enhanced MRAV

☆Financial disclosure: N/A.

*Corresponding author. Tel.: +1 313 758 0065; fax: +1 313 758 0068. sethisea@gmail.com (S.K. Sethi).

1. Introduction

Recently, Zamboni et al. postulated that the condition known as chronic cerebrospinal venous insufficiency (CCSVI) is prevalent in the MS population and influences the development or exacerbation of the disease course [1]. CCSVI can be described as blood flow obstruction within the primary extracranial venous drainage. The obstruction may be due to stenosis or extrinsic compression of the internal jugular veins (IJVs) [2,3]. Research has shown that congenital malformations and intraluminal venous anomalies may play a role in CCSVI and MS [3–6].

This work reports on two MR scanning methods, 2D time-of-flight (TOF) MRV and 3D dynamic contrast enhanced (CE) MRAV, both of which show strong promise for evaluating the extracranial venous system. In 2D TOF-MRV, blood flow is used as the intrinsic contrast agent and signal is based on an in-flow effect. 3D CE MRAV uses a T1-shortening contrast agent to enhance intraluminal signal.

In 2D TOF-MRV, the signal in the vessel depends on the flow up to a threshold speed defined by the slice thickness (mm) divided by the repetition time (ms). Vessels are best seen when they are orthogonal to the 2D plane, as in-plane vessels will generally have a loss of signal due to saturation effects [7,8]. Large vessels can be visualized easily and smaller vessels such as the paraspinal veins and dural sinuses can be seen as well. From these data, anatomical assessments can be made and cross-sectional area (CSA) can be measured to calculate the degree of stenosis. The high in-plane resolution available in this technique makes it a reliable method for measuring the caliber of all the major vessels in the slice of interest [9]. On the other hand, the dynamic (time-resolved) 3D CE MRAV scan is performed coronally before during and after injection of a T1-shortening contrast agent [10]. Some of the advantages of 3D CE MRAV include: high quality anatomical images of the arteries alone in the arterial phase, both arteries and the veins in the venous phase, delayed enhancement when obstructed flow is present, independence of the signal to the presence of various flow patterns, the ability to image small and tortuous vessels and reasonably short acquisition times for each 3D acquisition. There have been conflicting reports about the usefulness of MRV [2,3,10–15]. Therefore, the purpose of this study is to compare the 2D TOF-MRV and 3D CE MRAV and provide information on their usefulness for evaluating the structure of the venous system of the neck.

2. Materials and methods

Data were collected with a specific CCSVI protocol which included dynamic 3D CE MRAV and 2D TOF-MRV sequences (see Appendix I and II for parameters). Patients and healthy controls were passively recruited at two different imaging sites and the data were analyzed retrospectively. One-hundred seventy MS patients (118 female, average age: 50 years, 52 male, average age: 49 years; 87 relapsing–remitting, 39 primary progressive, and 44 secondary progressive) were imaged at Synergy Health Concepts (site 1) in San Diego, CA and 40 healthy controls (HCs) (23 female, average age: 40 years, 17 male, average age: 39 years) were imaged at Wayne State University (site 2) in Detroit, MI. All MS patients seeking possible treatment for CCSVI who received MRI scanning were included. MS diagnosis was made clinically with radiological confirmation. Both MS and healthy controls were excluded if they had history of major illness such as diabetes, chronic renal disease, neurological disorder(s) other than MS, or substance abuse. Institutional review board approval was obtained to process de-identified data from each site.

For site 1, a 3 T Signa HDxt scanner (GE Healthcare, Milwaukee, Wisconsin) with an eight channel head/neck coil arrangement was used for scanning the MS patients. For site 2, a 3 T Siemens Verio scanner with a sixteen channel head/neck coil arrangement was used to scan

the HCs. The subject was first scanned with the 2D TOF-MRV sequence and then positioned at the center of a head/neck coil arrangement in preparation for contrast medium injection. A contrast agent Magnevist [Bayer, Wayne, New Jersey] at site 1 and OptiMARK [Covidien, Hazelwood, Missouri] at site 2, both with 0.2 mL/kg [0.1 mmol/kg], was then injected and 3D MRAV data were acquired for 25 [15] time points. A saline bolus of equal contrast volume was injected after the contrast agent was injected.

The software "signal processing in nuclear magnetic resonance" (SPIN, Detroit, Michigan) was used for image review and data processing. The anatomical assessment of the cervical venous system included the identification of: stenosis, diffuse stenosis, carotid ectasia, atresia, aplasia, enhancement delays (3D CE MRAV), banding (2D TOF-MRV) and inhomogeneous signal (especially in 2D TOF-MRV) of the internal jugular veins (IJV). The cross-sectional areas of the vessel lumen (IJV) were measured at three different locations of the neck (C2/C3, C5/C6, and C7/T1).

Subjects were classified into the stenotic group if at least one of the following criteria was met [11]: atresia, which is abnormal closing or absence of the vessel, aplasia, which is defective development or congenital absence of the vessel, or diffuse stenosis in which the vessel is stenotic through its entire length. A CSA value less than 25 mm^2 at C7/T1 and C5/C6, or less than 12.5 mm^2 at the C2/C3 level [11] was considered stenotic. Carotid ectasias were noted if the carotid artery's course compressed the IJV and were marked as stenotic only if the resulting caliber of the compressed IJV was less than 25 mm^2 in both 3D CE MRAV and 2D TOF-MRV. All others were classified in the non-stenotic group. Paired student t-tests were done to show differences in 3D CE MRAV and 2D TOF-MRV CSA values in both IJVs, and at all three neck levels (Appendix IVa and IVb). Scatter plots showing 3D-measured CSA vs. 2D-measured CSAs have also been provided (Appendix Va and Vb).

The data from both sites were processed by six trained raters. For the IJV CSA measurements, the axial 2D TOF-MRV, and axial-reformatted 3D CE MRAV slices were matched to a localizer image which shows the exact level of the spine. Manual contours were defined by trained observers. Inter- and intra-rater variability was assessed by using a multiple-way analysis of variance with a randomized complete block design (Appendix III). Variability by processing time and neck level (C7/T1, C5/C6, and C2/C3) was also assessed. A significance level of $P \leq 0.05$ was used to determine whether inter- and intra-rater variability was significant using the null hypotheses that the inter- and intra-rater factor effect equals 0 [12].

3. Results

Of the 170 MS patients, 93 (55%) with 3D CE MRAV and 103 (61%) with 2D TOF-MRV showed stenosis in at least one IJV. A breakdown of the stenotic cases and signal classifications is shown in Table 1. A total of 6 [21] cases showed a loss of signal in the right IJV (RIJV) [left IJV (LIJV)] in the 3D CE-MRAV at any of the three levels. In the 2D TOF-MRV, an additional 3 [15] people showed signal loss in the RIJV [LIJV]. Of the total 1020 CSAs (170 cases × 3 levels × 2 sides) in the MS population, 37 (3.63%) CSAs showed no visible signal in 3D CE MRAV, while 68 CSAs (6.67%) showed no visible signal in 2D TOF-MRV. There was only one case which showed signal in the 2D TOF-MRV where there was no signal in 3D CE MRAV but the flow was very low (0.05 ml/s, flow quantified using PC-MR images) [11]. In the HC group, signal was visible for all neck levels in both RIJV and LIJV in both 2D TOF-MRV and 3D CE MRAV data.

In the MS group, the 3D CE MRAV data showed filling delays in seven (4%) cases in the LIJV and three (2%) cases in the RIJV. Of the stenotic-MS group, two (1%) instances of aplasia were noted in the 3D data. A total of 39 atresias were seen in the 3D data as follows: two in the right C7/T1 level, six in the left C7/T1 level, three in the right C5/C6 level, nine in the left C5/C6 level, five in the right C2/C3 level, and fourteen in the left C2/C3 level. The 3D CE MRAV data showed 33 bilateral stenoses, 18 RIJV-only stenoses, and 42 LIJV-only stenoses. The 2D TOF-MRV data showed 39 bilateral stenoses, 27 RIJV-only stenoses, and 37 left IJV-only stenoses. In the HC group, the 3D data showed one stenosis at the C7/T1 level in the LIJV, and one stenosis at the C5/C6 level in the LIJV. In the 2D data, there was one stenosis at the C7/T1 level in the RIJV, one stenosis at the C7/T1 level in the LIJV, and two stenoses at the C5/C6 level in the LIJV. No atresias, diffuse stenoses, or carotid ectasias were seen in the HC group with either the 3D or 2D methods.

Table 2 shows the average CSA values for stenotic and non-stenotic MS and HC groups measured with 3D CE MRAV and 2D TOF-MRV. The CSAs of the RIJV and LIJV from the 3D CE MRAV data show larger CSAs on average compared to the 2D TOF-MRV data in both MS patients and HCs.

Generally, we found that the 3D CE MRAV revealed the IJVs better than the 2D TOF-MRV. Figs. 1 to 3 provide example images of the differences and similarities in the delineation of the extracranial venous system between these two methods. Paired student t-tests show that the 3D data reported higher CSA measurements compared to 2D data at all three neck levels, in both RIJV and LIJV, in MS and HC groups. Data for MS types are also reported in Tables 3, 4a, and 4b.

In the 3D CE MRAV data, carotid ectasias were noted in both IJVs (Fig. 1). Six ectasias were seen in the RIJV and twenty-one were seen in the LIJV, with one case having bilateral ectasia. Dilation, in which the CSA of the IJV is greater than 250 mm^2, was also seen in MS patients and HCs in both scans and in both vessels. In the MS group, 11 dilation cases were seen in 3D CE MRAV and five were seen in 2D TOF-MRV. In the HCs, three dilation cases were seen in 3D CE MRAV and four were seen in 2D TOF-MRV.

Another example where the 3D CE MRAV showed much more detail than the 2D TOF-MRV data is shown in Fig. 2. The coronal 3D CE MRAV MIP image reveals the outline of the LIJV (Fig. 2A, B, and D), but the 2D TOF-MRV does not show any signal for the corresponding section (Fig. 2C and E). Fig. 3 shows an example of delayed enhancement of the LIJV in the 3D CE MRAV (A–C), and a corresponding banding pattern in 2D TOF-MRV (D).

3.1. Inter-rater Variability

The three-way analysis of variance showed that inter-rater variability was not significant for the IJV CSA measurements either by rater or by day (Appendix III).

4. Discussion

There are several studies indicating that cervical venous anatomy can be delineated noninvasively using 2D TOF-MRV as well as 3D CE MRAV [2,3,11,13–16]. In this paper, we have focused on the IJVs since they are the major carriers of extracranial venous drainage. A variety of structural abnormalities have been seen in the 170 MS patients studied including: atresia, stenosis, diffuse stenosis, aplasia, dilation, etc. The critical difference between the two sequences is that the 2D TOF-MRV sequence is sensitive to slow flow even though it does not measure flow directly. For example, the 2D TOF-MRV image may show a crescent shape in the upper IJVs whereas the 3D CE MRAV may show a

circular cross-section. This happens because of the rapid flow out from the sigmoid sinus that leads to a jetting down one side of the vessel so that the rapid flow generates a high signal in the 2D method at the edge of the vessel. On the other hand, the contrast diffuses in a relatively uniform manner within the blood tissue and shows the complete CSA of the vessel. Therefore, one might misinterpret this crescent jetting as abnormal when in fact it is likely just a normal flow variant. That is not to say that these patterns of narrowing, crescent shapes, flow down one side of the vessel, etc. are not also seen in 3D, sometimes they are seen. The only means to uniquely identify the meaning of these patterns seen in these magnitude images is to image the flow itself [11,13,17]. In a similar study, Mctaggart et al. [15] have recently reported that MS patients have greater IJV flattening and a trend toward more non-IJV collaterals than healthy subjects. Although we observed flattened and crescent shaped IJVs in our data in both MS patients and HCs, we did not quantify those criteria.

Conversely, a vessel may show no signal in both methods. This may be indicative of several things: anatomically, the vessel may be stenosed or occluded, abnormally closed (atresia) or developed (aplasia); there may be flow abnormalities such as no flow, or retrograde flow, or the slice in question may be subject to a banding or zipper artifact [7]. Lack of signal in 3D CE MRAV typically gets classified as stenosis because the contrast agent does not fill that area, so anatomically the vessel may be closed, extrinsically compressed, malformed, absent, or may have some intraluminal defect. No signal in 2D TOF-MRV is not as clear because slow flow will not generate signal even if the vessel is present, so the vessel cannot be assumed to be stenotic. Another interesting finding in the 2D TOF-MRV data is the banding artifact. If this occurs in all vessels it is likely due to swallowing or motion. There were several cases with contrast enhancement delay in the 3D CE-MRAV as well as a banding pattern in the 2D TOF-MRV as seen in Fig. 3. Over the series of the time-resolved 3D CE MRAV data, the RIJV fills but the LIJV does not until a later time point. The 2D TOF-MRV data show a banding pattern that extends the length of the LIJV until the confluence of the LIJV with the brachiocephalic vein (this could indicate that the origin of the flow problem is a malfunctioning valve for example).

Caliber reduction, pinpoint stenosis, and flattening are also observed in 3D CE MRAV, and have been observed in past studies [2,3,16]. One advantage of the 3D CE MRAV is that the vessel will show even if there is a disturbance in the flow pattern and it is less subject to de-phasing compared to the 2D TOF-MRV. So anatomically, the vessel may be present but there may be a flow-related problem (turbulence or slow flow). This may explain why the cross-sectional areas in the 2D TOF-MRV are less than those in the 3D CE MRAV as shown in Table 2. The resolutions for 2D TOF-MRV are also higher than the 3D CE MRAV resolutions for both sites, so this may also be a factor for the values of the CSAs being different.

In the HCs, signal was seen 100% of the time in both the 2D and 3D data. With respect to 2D data, this may be because the flow within the jugular vein may always be fast enough. With respect to 3D data, this may be because the HC jugular anatomy does not show as many stenotic characteristics as the MS group (see Table 1). 2D TOF is more sensitive to irregular flow patterns than 3D CE MRAV. In the case where there is reflux flow, only the unsaturated flow in the caudal direction will show signal in the 2D TOF-MRV, while the 3D CE MRAV signal will show signal for the entire lumen of the vessel.

Although we chose to use a fixed area for stenosis of 25 mm^2 for the C5-T1 neck levels, and 12.5 mm^2 for the C2–C3 neck levels, other authors have recommended a cutoff for stenosis of ≤30 mm^2 [1]. This choice was originally made based on the CSA falling below 1/3 of the area associated with a vein of diameter 1 cm [11]. Since jugular veins are not of consistent diameter as are the common carotid arteries for example, choosing a percentage variation of

a jugular vein is not a viable option. Therefore, we chose a fixed threshold at the different levels of the neck based on the average geometry seen in these areas.

Jugular stenosis/compression is generally seen at C2/C3, C4/C5, and C5/C6 cervical levels. At the C1–C3 level, compression of the IJV by the transverse process has been reported, as well as by the jugular foramen, hyoid bone, and styloid process [18]. Carotid bulb/carotid ectasias are generally seen at C4/C5 where the common carotid artery bifurcates, and C5/6 compressions may be due to the IJV being between the sternocleidomastoid muscle and the omohyoid muscles. What is notable is the average CSA values of the stenotic-MS group vary less between neck levels than the non-stenotic MS group and the HCs (Table 2). Lower CSA values have been linked to lower jugular outflow in previous research [11].

Both MR imaging techniques are less invasive than catheter venography and less operator-dependent than ultrasound. Both techniques are able to evaluate easily and globally the anatomic and morphologic features of the intracranial and extracranial venous system [2,3,11,14,15,19]. In 2D TOF-MRV, the in-flow of unsaturated spins provides for the potential of a strong signal of the blood relative to background tissue. For flow less than some threshold value the signal will be dependent on that flow, while above that threshold the signal will remain constant [20]. On the other hand, variations in the in-flow can generate flow-related pulsatility and ghosting artifacts. So, it is not unusual to have variable signal or loss of signal in the 2D TOF-MRV images [8]. These difficulties will not be encountered in 3D CE MRAV because the presence of a contrast agent leads to a more flow-independent signal.

We observed in many instances that the IJV shows banding (Fig. 3) and inhomogeneous signal in 2D TOF-MRV. Venous morphology and size depend upon the intrathoracic pressure, cardiac status, and compression from surrounding adjacent structures [21–24]. Morphologic changes of IJV could occur due to swallowing movements, different positioning of the head and neck, different respiratory phases during sequence acquisition, physiologic stenosis of the left brachiocephalic vein during regular breathing in the supine position [25–29].

Some of the drawbacks of both MR venographic methods include: the lack of sensitivity and resolution to view intraluminal abnormities that may be present in the MS population; the lower acquisition speed compared to ultrasound; the healthy volunteers were collected at a separate site; data observation for site 2 was not blinded, however the data from site 1 were. It would be prudent to blind the data for future analysis; and healthy controls tended to be younger on average. In data observation, the 3D data for both sites were reformatted which altered the observed resolution particularly for site 1 from $0.6 \times 0.6\ mm^2$ to $0.6 \times 2.0\ mm^2$ which may have contributed to an overestimation of the CSAs for that sequence at that site. Despite these disadvantages, we are still comparing the same two methods in each population (whether MS patients or volunteers) acquired on the same scanners; the sequences used were identical between the scanners; and the principles behind each method remain the same between scanners.

5. Conclusions

Both 2D and 3D MRV techniques provide complementary information about the anatomy and flow characteristics when imaging extracranial venous vessels. 3D CE MRAV provides a better representation of the vessel anatomy while the 2D TOF provides the potential for accurate cross-sectional measurements and can provide an indication of abnormally slow flow. For future studies related to CCSVI, it would be prudent to include 2D flow information to quantify and corroborate the 2D TOF information.

Acknowledgments

The authors would like to acknowledge Dr. Wei Feng for assistance with statistical analysis, and the following for their assistance with processing the data: Shwetha Namani, Ashwini Revelli, Vinay Kumar, and Prashant Nukala. Research reported in this publication was supported by the National Heart, Lung, And Blood Institute of the National Institutes of Health under Award Number R42HL112580. The content is solely the responsibility of the authors and does not necessarily represent the official views of the National Institutes of Health.

Abbreviations

CSA	cross-sectional area
HC	healthy control
IJV	internal jugular vein
CE	contrast-enhanced

References

1. Zamboni P, Galeotti R, Menegatti E, et al. Chronic cerebrospinal venous insufficiency in patients with multiple sclerosis. J Neurol Neurosurg Psychiatry. 2009; 80:392–9. [PubMed: 19060024]
2. Zivadinov R, Lopez-Soriano A, Weinstock-Guttman B, et al. Use of MR venography for characterization of the extracranial venous system in patients with multiple sclerosis and healthy control subjects. Radiology. 2011; 258:562–70. [PubMed: 21177394]
3. Zivadinov R, Galeotti R, Hojnacki D, et al. Value of MR venography for detection of internal jugular vein anomalies in multiple sclerosis: a pilot longitudinal study. AJNR Am J Neuroradiol. 2011; 32:938–46. [PubMed: 21474626]
4. Simka M, Kostecki J, Zaniewski M, et al. Extracranial Doppler sonographic criteria of chronic cerebrospinal venous insufficiency in the patients with multiple sclerosis. Int Angiol. 2010; 29:109–14. [PubMed: 20351666]
5. Al-Omari MH, Al-Bashir A. Internal jugular vein valve morphology in the patients with chronic cerebrospinal venous insufficiency (CCSVI); angiographic findings and schematic demonstrations. Rev Recent Clin Trials. 2012; 7:83–7. [PubMed: 22338622]
6. Nicolaides AN, Morovic S, Menegatti E, et al. Screening for chronic cerebrospinal venous insufficiency (CCSVI) using ultrasound: recommendations for a protocol. Funct Neurol. 2011; 26:229–48. [PubMed: 22364944]
7. Ayanzen RH, Bird CR, Keller PJ, et al. Cerebral MR venography: normal anatomy and potential diagnostic pitfalls. AJNR Am J Neuroradiol. 2000; 21:74–8. [PubMed: 10669228]
8. Spritzer CE. Progress in MR imaging of the venous system. Perspect Vasc Surg Endovasc Ther. 2009; 21:105–16. [PubMed: 19640860]
9. Muhs BE, Gagne P, Wagener J, et al. Gadolinium-enhanced versus time-of-flight magnetic resonance angiography: what is the benefit of contrast enhancement in evaluating carotid stenosis? Ann Vasc Surg. 2005; 19:823–8. [PubMed: 16200470]
10. Korosec FR, Frayne R, Grist TM, et al. Time-resolved contrast-enhanced 3D MR angiography. Magn Reson Med. 1996; 36:345–51. [PubMed: 8875403]
11. Haacke EM, Feng W, Utriainen D, et al. Patients with multiple sclerosis with structural venous abnormalities on MR imaging exhibit an abnormal flow distribution of the internal jugular veins. J Vasc Interv Radiol. 2012; 23:60–68. e61–63. [PubMed: 22221473]
12. Montgomery, DC. Design and analysis of experiments. New York: John Wiley; 2001.
13. Feng W, Utriainen D, Trifan G, et al. Quantitative flow measurements in the internal jugular veins of multiple sclerosis patients using magnetic resonance imaging. Rev Recent Clin Trials. 2012; 7:117–26. [PubMed: 22356242]
14. Dolic K, Marr K, Valnarov V, et al. Intra- and extraluminal structural and functional venous anomalies in multiple sclerosis, as evidenced by 2 noninvasive imaging techniques. AJNR Am J Neuroradiol. 2012; 33:16–23. [PubMed: 22194367]

15. Zaharchuk G, Fischbein NJ, Rosenberg J, et al. Comparison of MR and contrast venography of the cervical venous system in multiple sclerosis. AJNR Am J Neuroradiol. 2011; 32:1482–9. [PubMed: 21757521]
16. Hojnacki D, Zamboni P, Lopez-Soriano A, et al. Use of neck magnetic resonance venography, Doppler sonography and selective venography for diagnosis of chronic cerebrospinal venous insufficiency: a pilot study in multiple sclerosis patients and healthy controls. Int Angiol. 2010; 29:127–39. [PubMed: 20351669]
17. Dake MD, Zivadinov R, Haacke EM. Chronic cerebrospinal venous insufficiency in multiple sclerosis: a historical perspective. Funct Neurol. 2011; 26:181–95. [PubMed: 22364939]
18. Seoane E, Rhoton AL Jr. Compression of the internal jugular vein by the transverse process of the atlas as the cause of cerebellar hemorrhage after supratentorial craniotomy. Surg Neurol. 1999; 51:500–5. [PubMed: 10321879]
19. McTaggart RA, Fischbein NJ, Elkins CJ, et al. Extracranial venous drainage patterns in patients with multiple sclerosis and healthy controls. AJNR Am J Neuroradiol. 2012; 33:1615–20. [PubMed: 22517280]
20. Potchen, EJ. Magnetic resonance angiography: concepts & applications. St. Louis: Mosby-Year Book; 1993.
21. Beddy P, Geoghegan T, Ramesh N, et al. Valsalva and gravitational variability of the internal jugular vein and common femoral vein: ultrasound assessment. Eur J Radiol. 2006; 58:307–9. [PubMed: 16352411]
22. Doepp F, Schreiber SJ, von Munster T, et al. How does the blood leave the brain? A systematic ultrasound analysis of cerebral venous drainage patterns. Neuroradiology. 2004; 46:565–70. [PubMed: 15258709]
23. Escott EJ, Branstetter BF. It's not a cervical lymph node, it's a vein: CT and MR imaging findings in the veins of the head and neck. Radiographics. 2006; 26:1501–15. [PubMed: 16973778]
24. Schreiber SJ, Lurtzing F, Gotze R, et al. Extrajugular pathways of human cerebral venous blood drainage assessed by duplex ultrasound. J Appl Physiol. 2003; 94:1802–5. [PubMed: 12524376]
25. Kudo K, Terae S, Ishii A, et al. Physiologic change in flow velocity and direction of dural venous sinuses with respiration: MR venography and flow analysis. AJNR Am J Neuroradiol. 2004; 25:551–7. [PubMed: 15090340]
26. Tanaka T, Uemura K, Takahashi M, et al. Compression of the left brachiocephalic vein: cause of high signal intensity of the left sigmoid sinus and internal jugular vein on MR images. Radiology. 1993; 188:355–61. [PubMed: 8327678]
27. Tseng YC, Hsu HL, Lee TH, et al. Venous reflux on carotid computed tomography angiography: relationship with left-arm injection. J Comput Assist Tomogr. 2007; 31:360–4. [PubMed: 17538279]
28. Uchino A, Nomiyama K, Takase Y, et al. Retrograde flow in the dural sinuses detected by three-dimensional time-of-flight MR angiography. Neuroradiology. 2007; 49:211–5. [PubMed: 17180368]
29. Yakushiji Y, Nakazono T, Mitsutake S, et al. Sonographic findings of physiologic left brachiocephalic vein compression in a case initially misdiagnosed as a left internal jugular vein thrombus. J Ultrasound Med. 2009; 28:253–8. [PubMed: 19168776]

Appendix I. MR Sequence Parameters for MS Patients (site 1)

Sequence	3D CE MRAV	2D TOF-MRV
Orientation	Coronal	Transverse
TE (ms)	1.32	6.7
TR (ms)	3.48	20
Flip angle (degree)	25	70
No. of partitions (Nz)	72	varies

Sequence	3D CE MRAV	2D TOF-MRV
FOV (mm × mm)	512 × 512	512 × 512
Imaging matrix (Nx × Ny)	320 × 256	288 × 192
Resolution (mm × mm)	0.6 × 0.6	0.43 × 0.43
Slice thickness (mm)	2.0	1.5

Appendix II. MR Sequence Parameters for HCs (site 2)

Sequence	3D CE MRAV	2D TOF-MRV
Orientation	Coronal	Transverse
TE (ms)	1.25	5.02
TR (ms)	3.065	29
Flip angle (degree)	20	60
No. of partitions (Nz)	64	varies
FOV (mm × mm)	340 × 255	320 × 256
Imaging matrix (Nx × Ny)	384 × 288	512 × 204
Resolution (mm × mm)	0.9 × 0.9	0.63 × 0.63
Slice thickness (mm)	0.9	3.0

Appendix III. Experimental Design for Inter-rater Variability Study

To assess the inter-rater variability for the IJV CSA measurements, a multiple-way analysis of variance with randomized complete block design was conducted. Three patients were randomly selected (from site 1) to test inter-rater variability in the IJV CSA measurements by six raters. The CSA for an IJV for each patient was measured in day 1 at three levels (C2/C3, C5/C6, and C7/T1) for both sequences (2D TOF MRV and 3D CE MRAV). The same raters then repeated the processing on the same cases after one week. A three-way analysis of variance was performed with the two factors being rater, and processing day. The rater factor represents inter-rater variability and the processing day factor variability.

Sequence	level	p-value: rater	p-value: day
2D	C2/C3	0.233	0.941
2D	C5/C6	0.051	0.199
2D	C7/T1	0.238	0.098
3D	C2/C3	0.059	0.221
3D	C5/C6	0.101	0.321
3D	C7/T1	0.421	0.155

Appendix IVa. Paired student t-tests between observed CSA (mm2) signal between 3D and 2D methods in the MS group (site 1)

Scan Type	R-T1		R-C6		R-C2	
	3D MRAV	*2D TOF*	*3D MRAV*	*2D TOF*	*3D MRAV*	*2D TOF*
Mean	97.6	72.8	86.3	66.6	69.6	48.7
Standard Deviation	76.0	64.9	56.8	43.2	35.9	28.2
Observations	165	165	162	162	163	163
Hypothesized Mean Difference	0		0		0	
df	164		161		162	
t Stat	9.80		9.9		12.8	
P(T ≤ t) one-tail	<0.01		<0.01		<0.01	

Scan Type	L-T1		L-C6		L-C2	
	3D MRAV	*2D TOF*	*3D MRAV*	*2D TOF*	*3D MRAV*	*2D TOF*
Mean	68.6	53.7	68.1	51.9	47.8	31.5
Standard Deviation	51.5	48.5	41.8	35.7	23.5	17.1
Observations	157	157	151	151	150	150
Hypothesized Mean Difference	0		0		0	
df	156		150		149	
t Stat	7.3		10.7		14.6	
P(T ≤ t) one-tail	<0.01		<0.01		<0.01	

Appendix IVb. Paired student t-tests between observed CSA (mm2) signal between 3D and 2D methods in the HC group (site)

Scan Type	R-T1		R-C6		R-C2	
	3D MRAV	*2D TOF*	*3D MRAV*	*2D TOF*	*3D MRAV*	*2D TOF*
Mean	162.5	144.5	143.5	122.6	82.7	75.7
Standard Deviation	62.6	63.8	61.2	57.6	32.9	31.0
Observations	40	40	40	40	40	40
Hypothesized Mean Difference	0		0		0	
df	39		39		39	
t Stat	5.2		8.0		3.4	
P(T ≤ t) one-tail	<0.01		<0.01		<0.01	

Scan Type	L-T1		L-C6		L-C2	
	3D MRAV	*2D TOF*	*3D MRAV*	*2D TOF*	*3D MRAV*	*2D TOF*
Mean	99.1	90.3	101.5	88.8	55.8	49.3
Standard Deviation	57.1	52.7	55.9	52.2	26.8	22.8
Observations	40	40	40	40	40	40
Hypothesized Mean Difference	0		0		0	
df	39		39		39	

Scan Type	L-T1		L-C6		L-C2	
	3D MRAV	*2D TOF*	*3D MRAV*	*2D TOF*	*3D MRAV*	*2D TOF*
t Stat	3.7		4.9		4.3	
P(T ≤ t) one-tail	<0.01		<0.01		<0.01	

Appendix Va. Scatter plots of the RIJV CSAs (mm2) of the 3D vs. 2D methods in MS and HCs

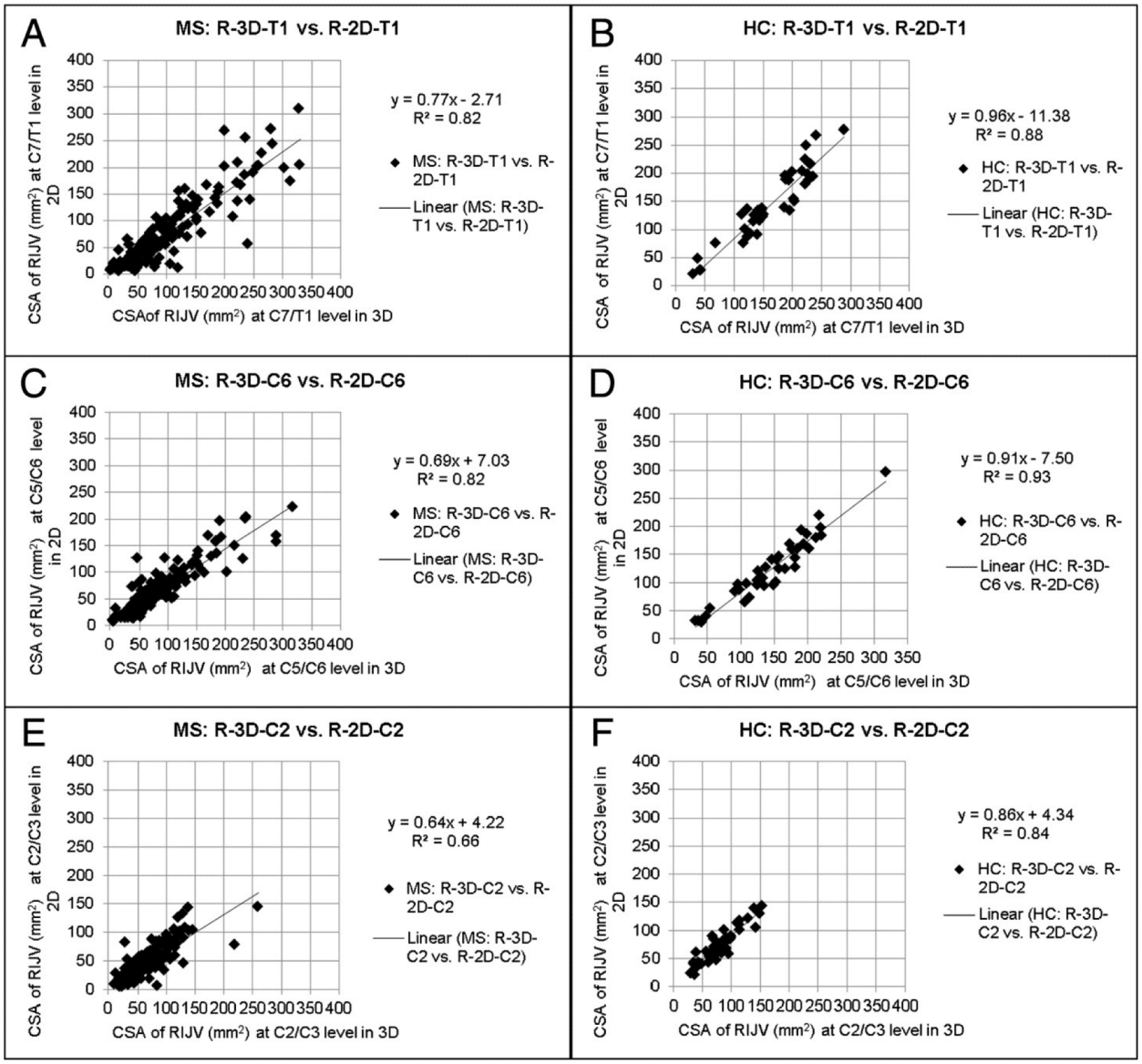

n = number of subjects in plots where signal is seen in both scans. A: number of plotted subjects where n = 165, B: n = 40, C: n = 162, D: n = 40, E: n = 163, F: n = 40.

Appendix Vb. Scatter plots of the RIJV CSAs (mm2) of the 3D vs. 2D methods in MS and HCs

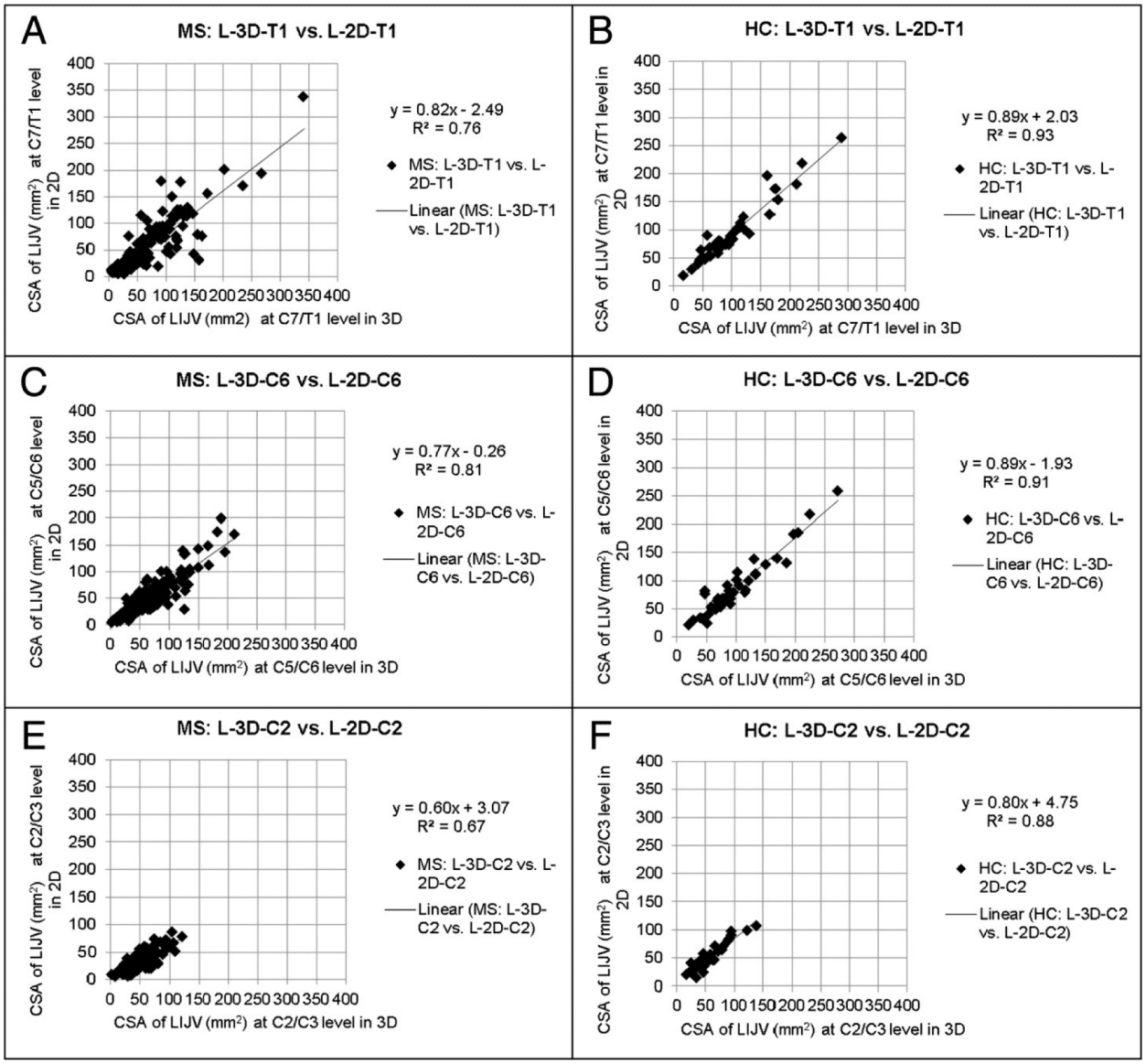

n = number of subjects in plots where signal is seen in both scans. A: n = 157, B: n = 40, C: n = 151, D: n = 40, E: n = 150, F: n = 40.

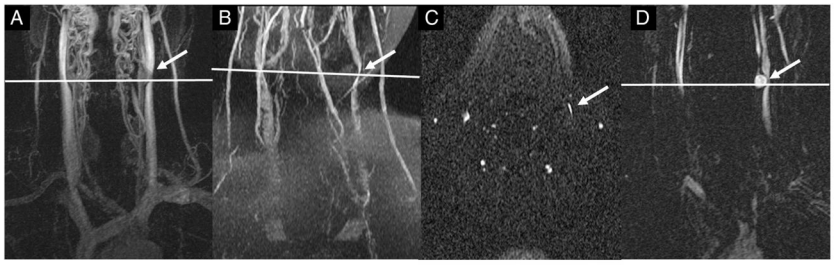

Fig. 1.

An example of the LIJV being compressed sufficiently by the left common carotid artery that it was considered stenotic. (A) A coronal maximum-intensity projection (MIP) (72 slices) of the time-resolved 3D CE MRAV showing a carotid ectasia (arrow in A). (B and C) Coronal and axial 2D TOF-MRV images where the LIJV (arrow) shows a stenosis at the C3–4 neck level. (D) 3D CE MRAV at the early venous phase clearly showing the carotid ectasia. The axial slice in C corresponds to the position line in A, B and D.

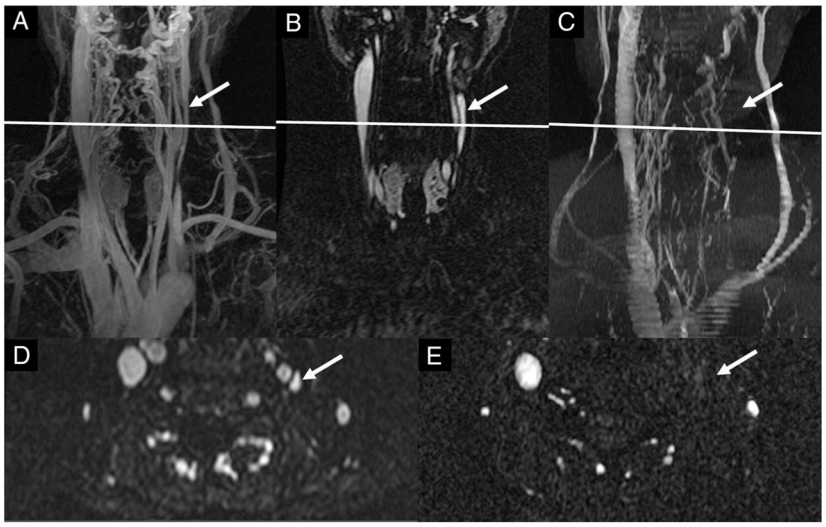

Fig. 2.

MS patient where the 3D CE MRAV shows very different results from the 2D TOF-MRV. (A) Coronal MIP (72 slices) of the time-resolved 3D CE MRAV where the LIJV is clearly visualized (left arrow). (B) Single slice image from the 3D CE MRAV. (C) MIP of the 2D TOF-MRV data where the LIJV shows no signal. (D) Axial slice of the 3D CE MRAV which corresponds to A and B and shows signal in the LIJV (arrow). (E) Axial 2D TOF-MRV slice which corresponds to C and shows no signal in the LIJV.

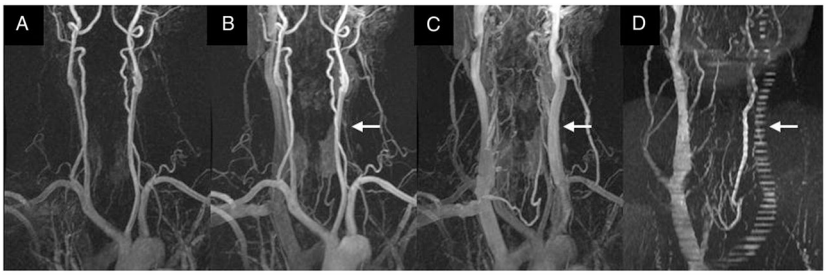

Fig. 3.

An example of banding in only one vessel for an MS patient. (A–C) Coronal 3D CE MRAV showing arterial phase time-point (A), early venous phase time-point (B), and late venous phase time-point (C). (D) An MIP of the 2D TOF-MRV. Over the series of the 3D CE MRAV data, the LIJV shows delayed enhancement. The late venous phase shows what appears to be a patent vessel. The corresponding 2D TOF-MRV shows a banding pattern in the LIJV which continues toward the brachiocephalic vein indicating slow or refluxed blood flow in those vessels.

Table 1

Stenosis, banding, and dilation classifications of the MS population, some stenotic cases include multiple criteria.

	3D	2D
R Diffuse	2	4
L Diffuse	8	7
R C7/T1 Stenosis	28	53
R C5/C6 Stenosis	11	26
R C2/C3 Stenosis	2	12
L C7/T1 Stenosis	33	54
L C5/C6 Stenosis	27	32
L C2/C3 Stenosis	9	16
R CA Ectasia	6	n/a
L CA Ectasia	21	n/a
R Enhancement Delay[a]	3	n/a
L Enhancement Delay[a]	7	n/a
Right Stenosis only	18	27
Left Stenosis only	42	37
R Aplasia	1	n/a
L Aplasia	1	n/a
Right C7/T1 Atresia	2	n/a
Left C7/T1 Atresia	6	n/a
Right C5/C6 Atresia	3	n/a
Left C5/C6 Atresia	9	n/a
Right C2/C3 Atresia	5	n/a
Left C2/C3 Atresia	14	n/a
Right Banding[a]	n/a	35
Left Banding[a]	n/a	51
Cases where (any level)	11	5
Bilateral Stenosis	33	39

[a]Were not included in the stenotic criteria.

Table 2

Average CSA values (in mm^2) for stenotic, non-stenotic MS and HC measured with 3D CE MRAV and 2D TOF-MRV.

		R-T1	R-C6	R-C2	L-T1	L-C6	L-C2	n
3D CE MRAV								
Stenotic MS	AVG	66.6	66.6	64.6	46.0	47.4	39.2	93
Stenotic MS	STD	60.0	49.4	35.0	36.5	31.2	21.5	93
Non-stenotic MS	AVG	132.2	105.4	73.3	90.5	87.1	54.8	77
Non-stenotic MS	STD	75.9	57.0	36.3	51.4	41.8	24.1	77
HC	AVG	162.5	143.5	82.7	99.1	101.5	55.8	40
HC	STD	62.6	61.2	32.9	57.1	55.9	26.8	40
2D TOF-MRV								
Stenotic MS	AVG	39.3	49.4	45.0	28.5	35.5	28.0	103
Stenotic MS	STD	34.4	32.7	27.8	24.9	20.6	15.9	103
Non-stenotic MS	AVG	123.1	91.2	54.2	87.3	73.7	36.6	67
Non-stenotic MS	STD	67.6	44.8	28.0	52.2	39.8	17.5	67
HC	AVG	144.5	122.6	75.7	90.3	88.8	49.3	40
HC	STD	63.8	57.6	31.0	52.7	52.2	22.8	40

Table 2 shows the averages and standard deviations of the CSAs of the right and left IJVs for the stenotic MS population, non-stenotic MS population, and HCs.

Table 3

Average CSA (mm^2) by MS type, sequence, and neck level.

	R-3D-T1	R-3D-C6	R-3D-C2	L-3D-T1	L-3D-C6	L-3D-C2
PP	89.8	76.3	62.8	63.1	64.8	49.5
	n = 38	n = 38	n = 39	n = 36	n = 38	n = 36
SP	110.3	93.5	73.4	76.0	76.8	50.0
	n = 42	n = 42	n = 42	n = 41	n = 39	n = 41
RR	93.3	83.7	69.0	64.4	61.9	43.9
	n = 87	n = 87	n = 85	n = 86	n = 83	n = 83

	R-2D-T1	R-2D-C6	R-2D-C2	L-2D-T1	L-2D-C6	L-2D-C2
PP	65.0	59.0	46.0	51.8	54.8	31.8
	n = 38	n = 37	n = 37	n = 36	n = 32	n = 33
SP	82.7	76.1	53.2	61.2	55.0	32.9
	n = 41	n = 40	n = 41	n = 38	n = 37	n = 38
RR	71.6	64.9	47.5	51.1	49.4	30.8
	n = 86	n = 86	n = 86	n = 83	n = 82	n = 79

Table 4a

Stenosis classifications by MS type using 3D CE MRAV.*

3D CE MRAV	PP	PP%	SP	SP%	RR	RR%
R Carotid Ectasia	0	0.0%	4	9.1%	2	2.3%
L Carotid Ectasia	2	5.1%	6	13.6%	13	14.9%
R Enhancement Delay	2	5.1%	4	9.1%	1	1.1%
L Enhancement Delay	1	2.6%	1	2.3%	1	1.1%
R Aplasia	0	0.0%	1	2.3%	0	0.0%
L Aplasia	1	2.6%	0	0.0%	0	0.0%
R T1 Atresia	1	2.6%	1	2.3%	0	0.0%
L T1 Atresia	2	5.1%	3	6.8%	1	1.1%
R C6 Atresia	1	2.6%	2	4.5%	0	0.0%
L C6 Atresia	1	2.6%	4	9.1%	4	4.6%
R C2 Atresia	1	2.6%	2	4.5%	2	2.3%
L C2 Atresia	5	12.8%	4	9.1%	5	5.7%
R Diffuse	0	0.0%	0	0.0%	2	2.3%
L Diffuse	3	7.7%	1	2.3%	4	4.6%
R T1 No signal	1	2.6%	2	4.5%	0	0.0%
R C6 No signal	1	2.6%	2	4.5%	0	0.0%
R C2 No signal	0	0.0%	2	4.5%	2	2.3%
L T1 No signal	3	7.7%	3	6.8%	1	1.1%
L C6 No signal	1	2.6%	5	11.4%	4	4.6%
L C2 No signal	3	7.7%	3	6.8%	4	4.6%
R T1 Stenosis	5	12.8%	7	15.9%	16	18.4%
R C6 Stenosis	4	10.3%	4	9.1%	3	3.4%
R C2 Stenosis	0	0.0%	1	2.3%	1	1.1%
L T1 Stenosis	7	17.9%	6	13.6%	20	23.0%
L C6 Stenosis	10	25.6%	5	11.4%	12	13.8%
L C2 Stenosis	2	5.1%	2	4.5%	5	5.7%
R Stenosis*	13	33.3%	15	34.1%	24	27.6%
L Stenosis*	20	51.3%	17	38.6%	38	43.7%

Magn Reson Imaging. Author manuscript; available in PMC 2014 February 24.

* The number of patients with stenosis independent of how many criteria were used.

Table 4b

Stenosis and banding classifications by MS type using 2D TOF-MRV.

2D TOF-MRV	PP	PP%	SP	SP%	RR	RR%
R Diffuse	1	2.6%	2	4.5%	1	1.1%
L Diffuse	1	2.6%	3	6.8%	3	3.4%
R T1 Stenosis	14	35.9%	12	27.3%	27	31.0%
R C6 Stenosis	6	15.4%	7	15.9%	13	14.9%
R C2 Stenosis	2	5.1%	4	9.1%	6	6.9%
L T1 Stenosis	14	35.9%	11	25.0%	29	33.3%
L C6 Stenosis	8	20.5%	5	11.4%	19	21.8%
L C2 Stenosis	4	10.3%	3	6.8%	9	10.3%
R T1 Stenosis	1	2.6%	3	6.8%	1	1.1%
R C6 Stenosis	2	5.1%	4	9.1%	1	1.1%
R C2 Stenosis	2	5.1%	3	6.8%	1	1.1%
L T1 Stenosis	3	7.7%	6	13.6%	3	3.4%
L C6 Stenosis	7	17.9%	6	13.6%	5	5.7%
L C2 Stenosis	6	15.4%	6	13.6%	8	9.2%
R Banding**	9	23.1%	11	25.0%	15	17.2%
L Banding**	12	30.8%	13	29.5%	26	29.9%
R Stenosis*	18	46.2%	18	40.9%	37	42.5%
L Stenosis*	24	61.5%	22	50.0%	44	50.6%

* The number of patients with stenosis independent of how many criteria were used.

** Banding not included in stenosis classification.